*Clays and Clay Minerals*, Vol. 46, No. 4, 436–445, 1998.

# DIAGENETIC TRANSFORMATION OF MAGNESITE PEBBLES AND COBBLES TO SEPIOLITE (MEERSCHAUM) IN THE MIOCENE ESKIŞEHIR LACUSTRINE BASIN, TURKEY

Ö. IŞIK ECE

Istanbul Technical University, Mining Faculty, Mineralogy-Petrography Section, Maslak 80626 Istanbul, Turkey

**Abstract**—Magnesite pebbles in Miocene lacustrine conglomerates in northwest Turkey have been partially to totally replaced by sepiolite. Only 5% of the magnesite pebbles have been converted to essentially pure sepiolite; the rest represent mixtures of magnesite and sepiolite. This process of sepiolitization is documented by X-ray diffraction (XRD), chemical, scanning electron microscopy (SEM) and Brunauer-Emmett-Teller (BET) techniques. These techniques show that the sepiolitization proceeds from the rim towards the core of the pebbles. The conglomerates, with pebbles of magnesite and ultramafic rocks, were deposited in a near-shore environment on the margin of a large Miocene lake with an ophiolitic substratum. The diagenetic transformation of magnesite to sepiolite is believed to have been caused by the interaction of mixed meteoric and lacustrine waters, which were undersaturated with respect to magnesite. The sepiolitization occurred during the highstands of the lake, when the near-shore conglomerates were flooded by the silica-rich lake waters. The pH of the water during the sepiolitization was probably on the order of 10.5–11.5. The sedimentary magnesite beds in the center of the Miocene basin show no sepiolitization, which is explained by the presence of pore water saturated with respect to magnesite.

The magnesite-sepiolite replacement process is chemically modeled as a 4-stage process from dimerization to polymerization.

**Key Words**—Diagenesis, Magnesite, Replacement, Sepiolite, Turkey.

## INTRODUCTION

"Meerschaum" is a specific name for the sepiolite nodules and pebbles in the Miocene Eskişehir basin in northwest Turkey. The physical properties of the meerschaum make it suitable for handcrafted pipes, chests and souvenirs. The Eskişehir lacustrine basin has the world's largest sepiolite deposits, which occur as sepiolite beds and pebbles (Akıncı 1967; Ece and Çoban 1994). Sepiolite beds were deposited in the central part of the basin, whereas sepiolite pebbles are found along the paleoshorelines of the Miocene basin. Stockwork-type magnesite deposits occur near the Miocene basin, where they formed during the ascent of $CO_2$-rich acidic hydrothermal waters along E-W trending growth faults and fractures through the serpentinites and peridotites, which constitute most of the basement of the basin.

Sepiolite veins have been reported as alteration products of ultramafic rocks formed by the effect of descending meteoric waters along cracks and fissures (Singer 1989). For example, Imai and Otsuka (1984) described sepiolite and xylotile occurring as veinlets in altered rocks of the Japanese serpentine belt. In addition, they reported authigenic palygorskite forming in veins and fissures along fault planes of Mg-rich carbonate rocks such as dolomite. In the Yunak region in central Turkey, Yeniyol (1986) described nearly pure sepiolite occurring as replacement veins in magnesite close to the topographic surface in sharp contact with the host serpentinite. Based on this field observation, Yeniyol and Öztunalı (1985) claimed that the sepiolite pebbles in the Yunak region were formed by the *in-situ* replacement of preexisting magnesite.

In this paper, shallowly buried (<100 m) strata with sepiolite pebbles and cobbles are investigated with emphasis on the diagenetic changes of magnesite minerals and the origin of sepiolite. The other aim of this paper is to explain why sedimentary magnesite beds, which are directly precipitated from lake waters in the central part of the Miocene lake, are not sepiolitized.

## GEOLOGIC SETTING

The best known and largest reserves of sepiolite pebbles and cobbles in the Eskişehir basin are located NE of Eskişehir, mainly in the Margı (Sepetçi-Taycılar) area (Figure 1). Minor deposits of sepiolite pebbles have been exploited in Nemli and Sarısu areas (Akıncı 1967). They occur in very poorly sorted conglomerate beds composed of pebbles and cobbles of altered ultramafic rocks, magnesite and sepiolite. These beds are directly underlain by the ophiolite complex of ophiolite melange, gabbro, pyroxenite, dunite and peridotite (Asutay et al. 1989). Miocene and younger E-W trending normal faults are common and have affected the Miocene sediments in the Margı and Nemli areas (Ece and Çoban 1994).

## METHODS AND STUDY

Samples were collected from shallow (<100 m) sepiolite underground mines. Hand-broken, dried clay chips, with fresh surfaces turned upward, were glued





https://doi.org/10.1346/CCMN.1998.0460408 Published online by Cambridge University Press

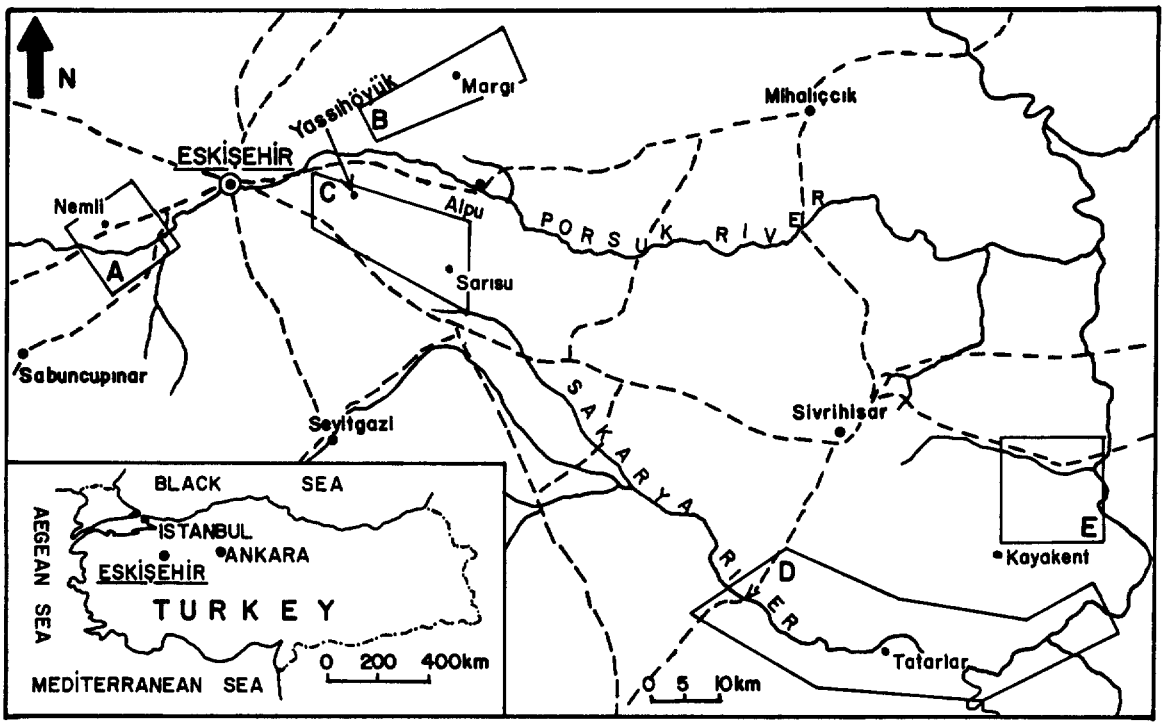


Figure 1. Index map of the lacustrine basin. Sepiolite nodules occur in areas A, B and C; sepiolite beds are abundant in areas D and E.

to sample holders and coated with a 200-Å thick Au-Pd film for SEM studies with a JEOL JSMT 330 model. The mineralogical composition of the samples was examined with a Philips 1140 XRD with Ni-filtered Cu$K\alpha$ radiation at a scanning speed of 1 °2θ/min. The identification of clay minerals was done on thermally treated samples, which were air-dried and ethylene-glycol-saturated for 12 h at 60 °C. For clay mineral analysis, smear glass samples were prepared on glass slides from the <2-μm clay fractions that were obtained by centrifuging (Gibbs 1965 and 1968). For chemical analysis, dried and powdered samples were melted in a crucible at 850 °C with 50% mixture of $K_2CO_3$ and $Na_2CO_3$, then dissolved in HCl. A Perkin-Elmer 3030 model atomic absorption spectrophotometer was used for the analysis of Al, Fe, Na and K: gravimetric method for the analysis of Si, ammonium oxalate precipitation method for that of Ca and diamonium hydrogen phosphate precipitation method for the analysis of Mg. For BET measurement, sorption of $N_2$ is enhanced by removal of water from channels by outgassing in vacuum at 70–80 °C using a Quanto Chrome Autosorb-I instrument.

## CLAY MINERALOGY

### XRD Studies

Based on data from randomly oriented samples, the stages of increasing sepiolitization of the parent rock magnesite are documented in Figure 2. The main magnesite reflections are 2.74, 2.10 and 1.70 Å, and they gradually disappear toward 12.52, 4.51, 2.57 and 2.27 Å as sepiolitization progresses. The details of the XRD patterns of pure sepiolite in the <2-μm fractions are reported by Ece and Çoban (1994). In this series, a weak and broad reflection, possibly that of hydroxide hydrate magnesium carbonate mineral ($Mg_5(CO_3)_4(OH)_24H_2O$), is found at 7.52 Å (130) (samples 2, 10, 9A and 9 in Figure 2). This broad reflection appearing initially at 7.52 Å shifts to 7.62 Å (031), as the 12.35 Å reflection (110) shifts to 12.52 Å in pure sepiolite samples (Figure 2), indicating that small amounts of hydroxide hydrate magnesium carbonate exist even in the strongly sepiolitized cobble of sample 2.

### Chemical Data

Sepiolitization was chemically investigated by analyzing individual magnesite-sepiolite pebbles, as well as by analyzing separately the cores and rims of some of the pebbles (Table 1). All magnesite and sepiolite samples have very low $Al_2O_3$, $Na_2O$, $K_2O$, $TiO_2$ and $Fe_2O_3$ contents, indicating an ultramafic origin. The pure magnesite sample contains 0.25% $SiO_2$ and about 47.5% MgO (sample 4 in Table 1). Among the strongly sepiolitized pebbles, the Ca, Si and Mg contents are not uniform, reflecting the presence of micron-sized magnesite crys-

https://doi.org/10.1346/CCMN.1998.0460408 Published online by Cambridge University Press

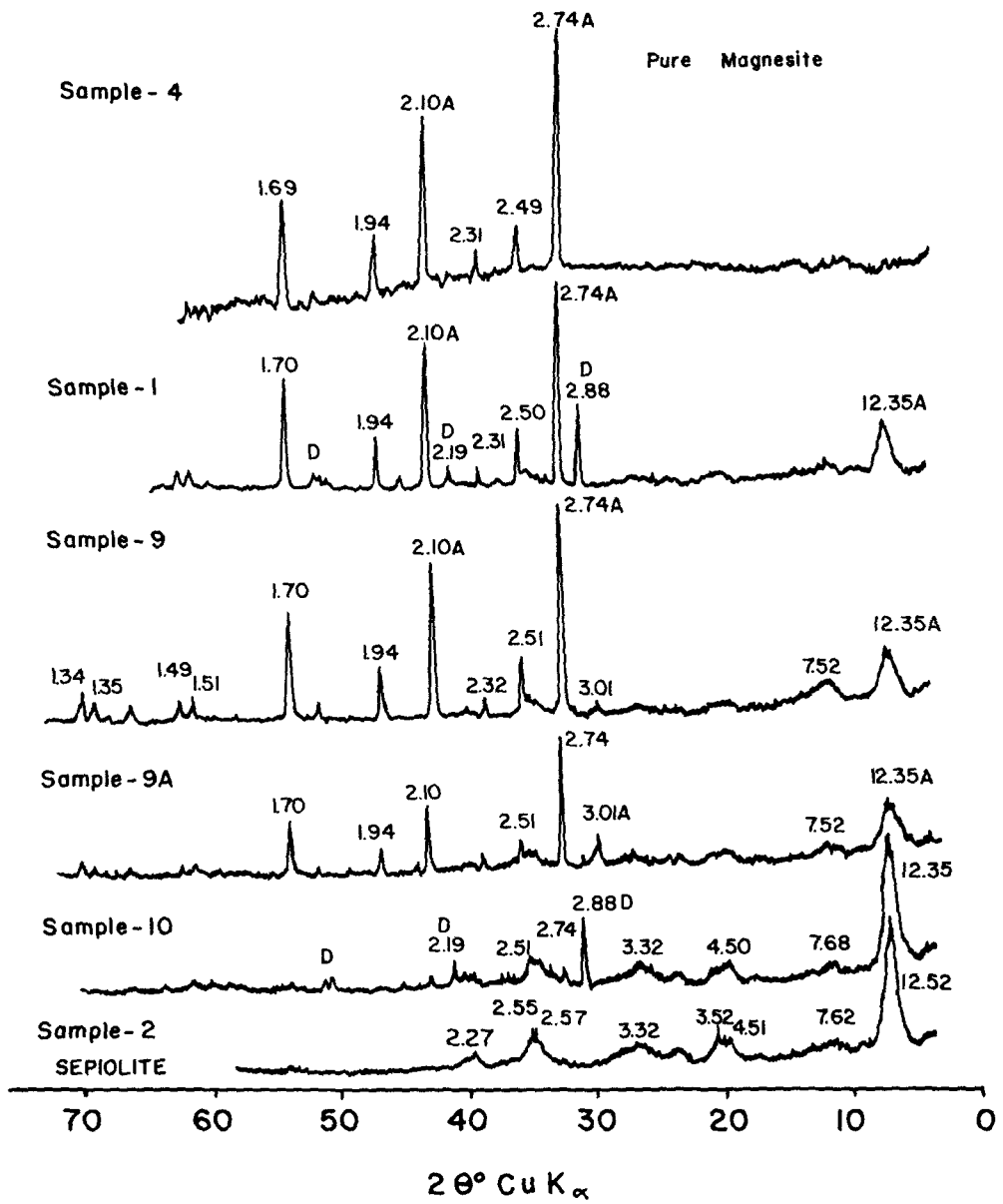


Figure 2. XRD patterns of randomly oriented powder samples of varying mixtures of magnesite and sepiolite. D = dolomite.

tals. In pebbles, where the core and surface compositions were separately analyzed (Table 1), $SiO_2$ content increases and MgO decreases from core to rim, indicating that magnesite dissolution and silica absorption—neomineralization—starts from the rim of the pebble.

Using the Brauner-Preisinger model (Jones and Galan 1988) for ideal sepiolite, the structural formulae of sepiolite pebbles are calculated as follows (Table 1):

Sample 12 $(Si_{11.96}Al_{0.04})(Mg_{7.63}Fe_{0.003}Ti_{0.003})_{7.64}$-$Na_{0.073}K_{0.06}Ca_{0.13}$

Sample 14 $(Si_{11.96}Al_{0.04})(Mg_{7.62}Ti_{0.02}Fe_{0.003})_{7.64}$-$Na_{0.07}K_{0.05}Ca_{0.13}$

Sample 15 $(Si_{12.0}(Mg_{7.55}Fe_{0.003}Ti_{0.018}Al_{0.034})_{7.60}$-$Na_{0.07}K_{0.068}Ca_{0.13}$

Sample 16 $(Si_{11.95}Al_{0.05})(Mg_{7.81}Fe_{0.04})_{7.85}$-$Na_{0.03}K_{0.01}Ca_{0.08}$

https://doi.org/10.1346/CCMN.1998.0460408 Published online by Cambridge University Press

Table 1. Chemical analyses of pebbles with varying amounts of magnesite and sepiolite. Samples 16, 12, 13, 14 and 15 are essentially pure sepiolite; 4 is magnesite; and the rest contain varying mixtures of both minerals.

| Sample No. | $SiO_2$ | $Al_2O_3$ | $Fe_2O_3$ | $TiO_2$ | CaO | MgO | $Na_2O$ | $K_2O$ | LOI |
|---|---|---|---|---|---|---|---|---|---|
| 16 s | 52.87 | 0.35 | 0.40 | — | 0.80 | 23.21 | 0.06 | 0.04 | — |
| 12 s | 60.20 | 0.35 | 0.04 | 0.07 | 0.79 | 25.77 | 0.24 | 0.26 | 12.10 |
| 13 s | 54.82 | 0.30 | 0.27 | — | 0.39 | 24.49 | 0.06 | 0.05 | — |
| 14 s | 60.10 | 0.30 | 0.04 | 0.07 | 0.63 | 25.91 | 0.23 | 0.26 | 12.05 |
| 15 s | 60.05 | 0.30 | 0.04 | 0.06 | 0.61 | 25.34 | 0.23 | 0.27 | 11.70 |
| 3A sm | 59.70 | 0.05 | 0.05 | — | 0.22 | 27.70 | 0.03 | 0.02 | — |
| 3B sm | 50.35 | 0.13 | 0.02 | — | 1.60 | 24.95 | 0.03 | 0.01 | — |
| 2C sm | 58.35 | 0.25 | 0.05 | 0.06 | 0.92 | 26.47 | 0.21 | 0.27 | 13.80 |
| 2R sm | 58.90 | 0.25 | 0.05 | 0.07 | 1.27 | 25.93 | 0.21 | 0.26 | 12.80 |
| 9C sm | 21.70 | 0.15 | 0.06 | — | 1.70 | 37.50 | 0.02 | 0.02 | — |
| 9R sm | 33.50 | 0.30 | 0.30 | — | 5.00 | 30.00 | 0.02 | 0.01 | — |
| 11C sm | 42.60 | 0.05 | 0.07 | — | 1.00 | 32.70 | 0.03 | 0.02 | — |
| 11R sm | 49.90 | 0.15 | 0.03 | — | 0.50 | 26.30 | 0.02 | 0.01 | — |
| 4 m | 0.25 | 0.08 | 0.02 | — | 1.00 | 47.50 | 0.02 | 0.01 | — |
| 8 sm | 22.00 | 0.10 | 0.24 | — | 1.30 | 37.00 | 0.03 | 0.01 | — |
| 10A sm | 52.30 | 0.38 | 0.16 | — | 3.00 | 26.95 | 0.02 | 0.02 | — |
| 10B sm | 50.80 | 0.25 | 0.05 | — | 1.60 | 24.15 | 0.03 | 0.01 | — |

Key: s = sepiolite, m = magnesite, sm = sepiolite-magnesite mixture, C = core, R = rim.


Figure 3. SEM photomicrographs of pure magnesite samples.

Sample 13 $(Si_{11.96}Al_{0.04})(Mg_{7.90}Fe_{0.02})_{7.92}$-$Na_{0.02}K_{0.01}Ca_{0.1}$

Samples 16 and 13 are selected from very pure sepiolites. Octahedral cation occupancy is in fact low, as seen in the structural formulae. Chemical heterogeneity is also observed in samples 3A and 3B, which show 2 different chemical compositions that were collected in the central part of the same cobble.

## SEM Studies

Magnesite-sepiolite transformation is documented step-by-step in SEM studies as shown in Figures 3, 4 and 5. Figure 3 shows magnesite rhombs in the pure magnesite sample. The incipient sepiolitization is illustrated in Figure 4, where sepiolite fibers, which form from the dissolution of magnesite, are thin and short (2–4 μm); as sepiolitization progresses, the sepiolite forms bundles of more elongate and thicker fibers (Figure 5). The gradual replacement of magnesite rhombs by sepiolite results in volume expansion, as also observed in the field. Cobbles show expansion-induced cracks and radiational growth on their surface. In later stages of this process, the conical-shaped cracks are filled by mud and thin dolomite crusts. As a result, the size and shape of the magnesite pebbles change during the sepiolitization. Magnesite contains ~48 wt% MgO and sepiolite, ~25 wt%. Hence, some of the Mg and all of the $Co_3$ are lost during replacement.

The solution film, which must accompany the magnesite-sepiolite replacement process, is not observed by SEM, possibly because its thickness is much less than the thickness of sepiolite fibers, which are themselves less than 0.1 μm thick. A concentric-shape replacement process, which occurs in the carbonate-ap-

https://doi.org/10.1346/CCMN.1998.0460408 Published online by Cambridge University Press

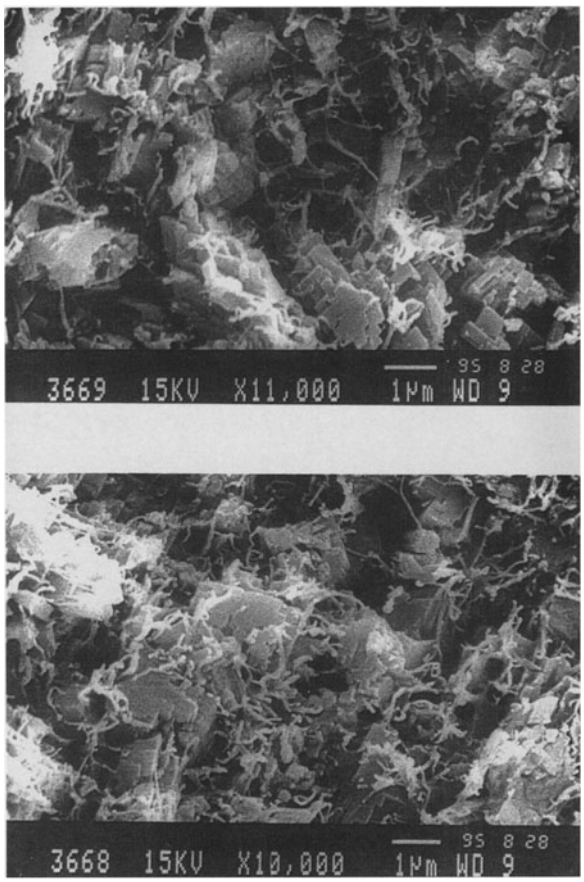


Figure 4. SEM photomicrographs of samples with magnesite and replacing sepiolite (fibers).

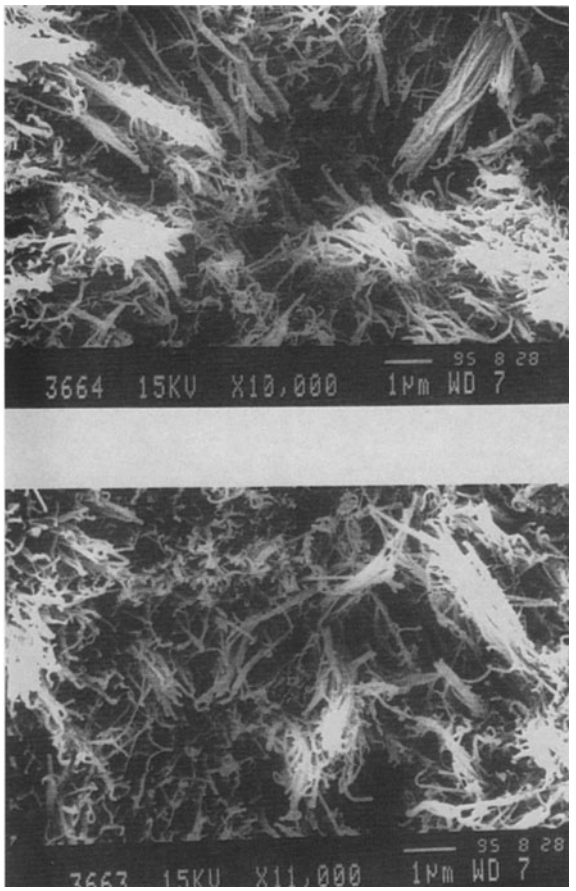


Figure 5. SEM photomicrographs of pure sepiolites showing bundles of tightly interwoven fibers. The bent tops of the sepiolite fibers are probably due to gravity and/or different zeta potential.

atite diffusion-replacement (Burnett 1977; Riggs 1979; Ece 1990), is not found in the magnesite-sepiolite transformation.

## Surface Area (BET) Studies

Surface area properties are important for catalytic reactions of sepiolites. The surface area in sepiolite depends on the size of the fibers as well as on the nature of the molecules (size, shape, polarity) used as sorbate to penetrate the intracrystalline channels (Jones and Galan 1988). Nitrogen cannot penetrate far into the channel structures and is predominantly adsorbed on external surfaces. "Microporosity", the inner surface area in the channels between the talc-like ribbons, is the major contribution to this adsorption process in sepiolite. The relationship between the BET surface area and the crystallinity of sepiolite is more complicated. The macropores within the fabric of sepiolite bundles play a part. Therefore, BET measurements are carried out to evaluate the catalytic potential of sepiolite and not to assess its crystallinity. However, this method also provides a good indication of the extent of sepiolitization, especially as magnesite has a much smaller surface area than sepiolite.

Nitrogen surface areas are calculated for the samples with essentially pure magnesite (sample 4), pure sepiolite (samples 10A, 12, 14 and 15) and magnesite-sepiolite mixtures (Table 2). Pure magnesite (sample 4) has 3.09 $m^2/g$ surface area, whereas pure sepiolite shows a surface area as high as 351.66 $m^2/g$. The other samples with magnesite-sepiolite mixtures give inter-

Table 2. BET results showing surface area measurements of pure magnesite (4), pure sepiolite (samples 10A, 12, 14 and 15) and samples with magnesite-sepiolite mixtures.

| Sample No. | BET surface area $m^2/g$ |
|---|---|
| 4 | 3.09 |
| 7 | 80.10 |
| 8 | 166.97 |
| 9R | 260.67 |
| 2R | 280.28 |
| 15 | 300.92 |
| 10A | 302.92 |
| 14 | 323.07 |
| 12 | 351.66 |

https://doi.org/10.1346/CCMN.1998.0460408 Published online by Cambridge University Press

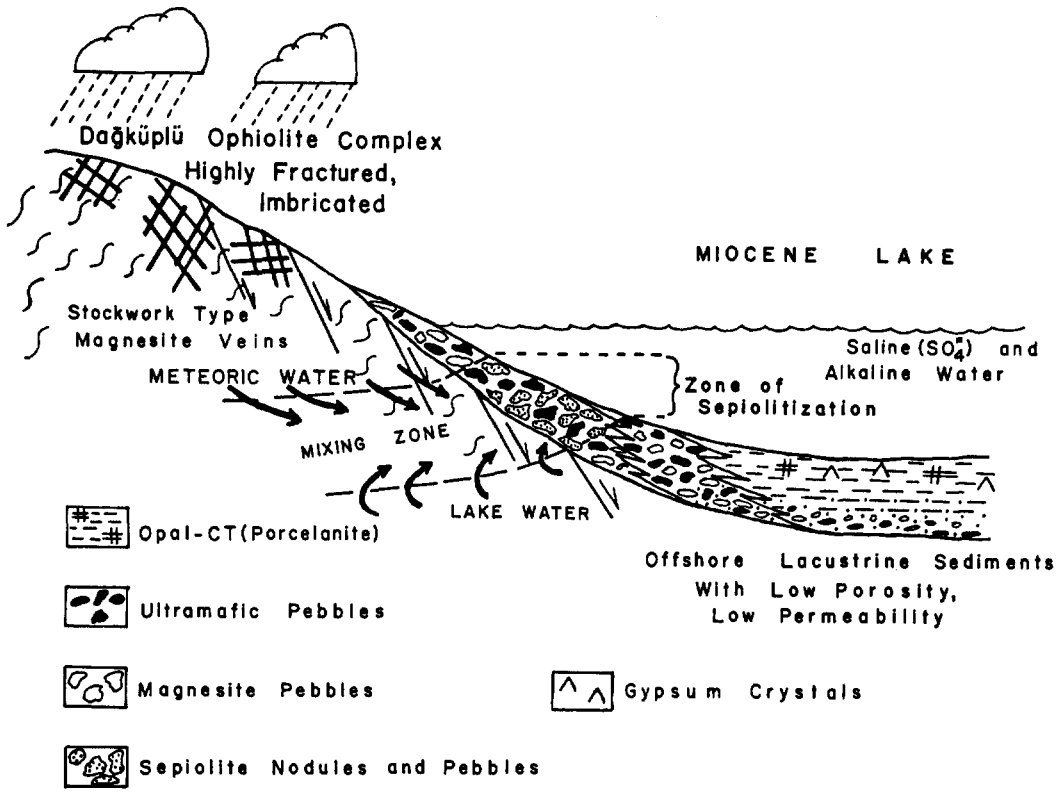


Figure 6. Generalized hydrogeologic model to explain the formation of sepiolite pebbles by replacement of the magnesite on the shores of the Miocene lake. The basement of the lake is made up of ophiolite. Modified from Knauth (1979).

mediate surface area values, showing that BET measurements indicate the general trend of sepiolitization. In comparison, nitrogen surface areas of commercial sepiolite beds of Spain range from 200 to 380 $m^2/g$ (Dandy 1968; Serratoga 1979). BET surface areas of 263 $m^2/g$ were reported for sepiolites from sedimentary sepiolite deposits of Vallecas-Vicalvaro in Spain (Belzunce et al. 1991), and those from Amboseli from Tanzania had BET surface areas of 316 $m^2/g$ (Dandy and Nadiye-Tabbiruka 1982). The Amboseli basin is famous because of kerolite occurrence and kerolite-sepiolite transformation. The higher surface areas (>300 $m^2/g$) shown by the Turkish sepiolites is probably due to the relatively small length of the sepiolite fibers, as documented by SEM microphotographs.

## GEOLOGIC MODEL AND DISCUSSION

A model explaining the sepiolitization process in a lacustrine Miocene environment is shown in Figure 6. The Miocene sediments, which accumulated as debris flow deposits on the margins of the lake, were predominantly made up of grains to blocks of serpentinite altered to various degree to Mg-smectite, chlorite, talc and amorphous silicates. These Mg-rich sediments were later subaerially exposed following a drop in the water level of the lake. During these lowstand episodes, gypsum and opal-CT were deposited in the central part of the lake, indicating that the lake water was saturated with Si. The flooding of the Si-rich water over the Mg-rich debris deposits on the paleoshore during a subsequent rise in the lake level resulted in the sepiolitization of the Mg-rich near-shore sediments (Figure 6). This process must have been aided by the introduction of fresh water from the ophiolitic substratum. The fluctuation in the water level of the lake probably occurred several times, resulting in several phases of sepiolitization. Si-rich saline lake water was mixed with ophiolite-origin freshwater in the mixed-water zone by buoyant circulation in phreatic zones beneath freshwater lenses. The main source of silica is geothermal waters ascending through highly fractured and faulted magmatic rocks and through an imbricated serpentinite body, mainly from underneath the lake. An additional silica source is diatomaceous oozes in lake water.

In the region of Margı (Kötükışla area), the economically important sepiolite zone (75–150 cm thick), with pebbles of sepiolite, magnesite and ultramafic rock, is both underlain and overlain by red silt and clays without any pebbles. The stronger porosity and permeability shown by the sepiolite zone, in comparison with the underlying and overlying clay-rich sed-

https://doi.org/10.1346/CCMN.1998.0460408 Published online by Cambridge University Press

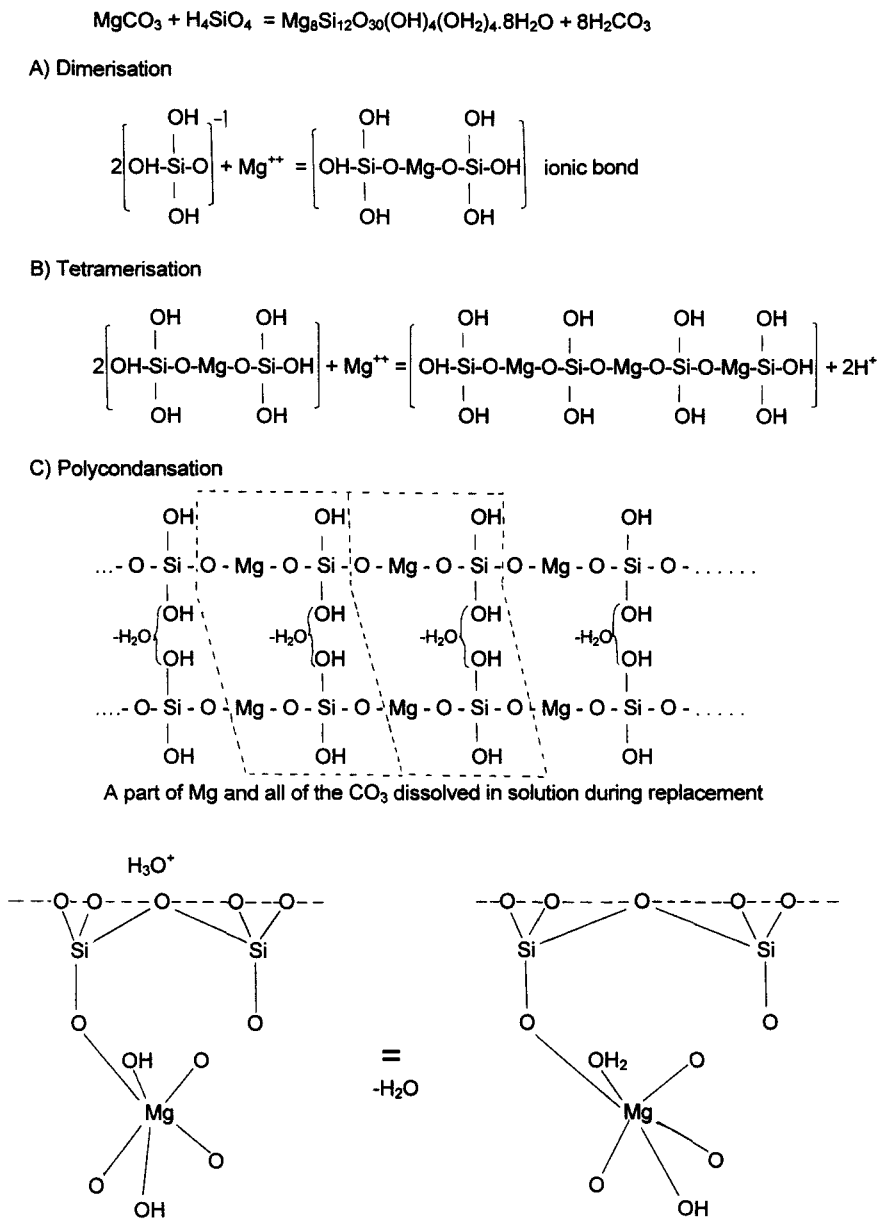


Figure 7. The proposed polymerization model to explain the sepiolitization process of magnesites. For explanation, see the text.

iments, makes it open for groundwater circulation (recharge area). The groundwater formed by the mixing of silica-poor meteoric (= ophiolitic) water and silica-rich alkaline and saline lake water on the margins of the paleoshore enhances the diagenetic replacement process.

A similar setting and process have been invoked to explain the origin of some nodular cherts in shallow marine limestone (Knauth 1979). According to Knauth (1979), if the mixed-water zone is closed with respect to $CO_2$, the zone might be undersaturated with respect to calcite, and if carbonate sediments contain silica sponges or other forms of soluble silica, then nodules of replacement chert form in the mixing zone. In the Eskişehir example, the analogy would be that in a system closed with respect to $CO_2$, the mixture of dilute ophiolite water (saturated with respect to magnesite) with lake water (saturated with respect to magnesite during very lowstand episode, but unsaturated during highstand episode) would be undersaturated with respect to magnesite, and pebbles of magnesite would be replaced by sepiolite. The observation that sepiolite

https://doi.org/10.1346/CCMN.1998.0460408 Published online by Cambridge University Press

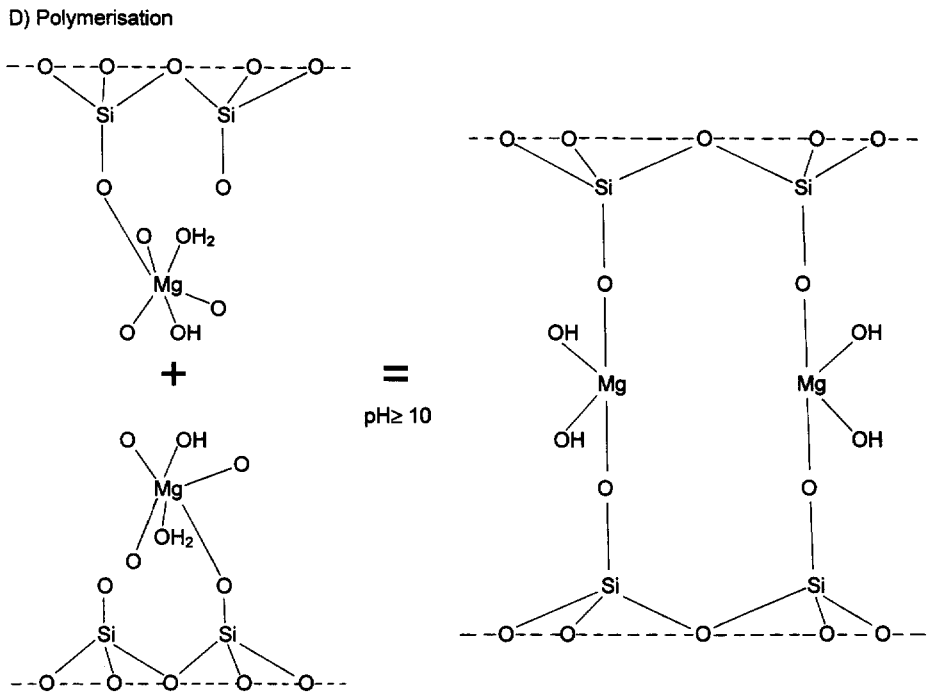


Figure 7. Continued.

does not replace bedded lacustrine magnesite is because lacustrine pore fluids are saturated with respect to magnesite.

In the Margı area, dolomitization increases in the mixing zone, as proposed earlier for dorag dolomitization in Wisconsin by Badiozamani (1973). Silicification occurring during mixing zone dolomitization would initially produce sepiolite nodules from magnesite nodules followed by the chertification of the nodules. However, an insufficient amount of silica was available during this process, as shown by the observation that only 5% of the pebbles exploited from underground operations are purely sepiolite; the rest are mixture of sepiolite and magnesite in different percentages. Therefore, this mixing zone is considered a silica-deficient water zone. Neal and Stanger (1985) reported that average chemical concentrations (mg/L) in Oman ophiolite sequence groundwaters vary as follows: pH = 11.2–11.6, $SiO_2$ = 1.0–4.0, Na = 226–257, K = 8.6–10.8, Mg = 0.15–0.47, Ca = 57.6–61.0, Cl = 306.4–361.6 and $SO_4$ = 16.8–23.3 ppm. As silicate dissolution is indicated, the release of Mg, Ca and OH to solution results in rising pH, and consequently the conversion of $HCO_3$ to $CO_3$.

Sepiolitization of magnesite pebbles is regarded as a 4-step process (Figure 7). These are A) dimerization, B) tetramerization, C) polycondensation and D) polymerization. The first process involves ionic bonding between Mg cations and the silicic acid brought together by the interaction of the magnesite pebbles and the ground water. In the tetramerization, the dimerization is enhanced to form longer chains with ionic bonds (Figure 7). This is accompanied by dehydration and decarbonization, whereby some of the Mg and all of $CO_3$ are lost from the structure. The $H^+$ bond will take place between tetrahedron and octahedron upon dehydration. During the polycondensation, the chains with ionic bonds come together to form loose sheet-like structures. In the last phase of polymerization, the structure becomes more coherent with a gradual change from ionic to covalent bond. The final step of this phase is the formation of the sepiolite structure consisting of alternating tetrahedral and octahedral layers.

According to Weaver (1989), in the presence of cations $Si(OH)_4$ polymerizes to form a tetrahedral sheet. The formation of the octahedral sheet of sepiolite is related to the formation of hydroxides. Cations in solution attract the negative end of water molecules and become hydrated $(Mg(H_2O)_6)^{2+}$. As the pH of solution and hydroxyl ion concentration increases, the hydroxyls progressively replace the molecules of water present in the layer of hydration:

$$(Mg(H_2O)_6)^{2+} + OH^{1-} = (Mg(H_2O)_5(OH))^{1+} + H_2O = \ldots = (Mg(H_2O)_4(OH)_2) + H_2O \quad [2]$$

Due to the large size and the high charge density of

https://doi.org/10.1346/CCMN.1998.0460408 Published online by Cambridge University Press

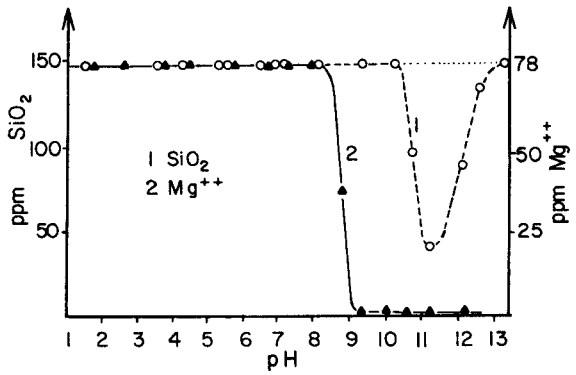


Figure 8. Solubility of amorphous silica and Mg in mixed solution as a function of pH. (After Wey and Siffert (1961).

Mg, the water molecules are more weakly bonded and can be completely replaced by hydroxyls relatively easily to form the hydroxide precipitates. Further, when Si is present it always coprecipitates with the hydroxide (Weaver 1989). The solubility of Si is a function of pH. At pH < 9, dissolved Si is present as monosilicic acid, $H_4SiO_4$, as long as the total concentration of silica in water is less than 100–140 mg/L $SiO_2$ at 25 °C. Silicic acid is a very weak acid, the first dissociation constant being $K = (H^+)(H_3SiO_4^{1-})/(H_4SiO_4) = 10^{9.9-}$. Hence, the solubility of silica is not affected by pH below 9, but greatly increases at higher pH values. At pH > 9, $H_4SiO_4$ dissociates to ($H_4SiO_4 = H_3SiO_4^{1-} + H^+$) its conjugate base $H_3SiO_4^{1-}$ and at pH > 11, $H_2SiO_4^{2-}$ will react with available cations in solution in order to form new silicate material. As most natural waters coming from ophiolite complex and some alkaline lakes have pH > 10, (in the range pH = 10.5–11.5), dimerization and tetramerization will begin after dissociation of $H_4SiO_4$ and by the presence of Mg.

The relation between the Mg and Si concentrations in an aqueous solution on the precipitation of Mg-Si-phases at various pH values is studied experimentally by Wey and Siffert (1961). In the presence of Mg, the solubility of Si decreases rapidly in the narrow pH range between 10 and 12 (Figure 8). At higher concentrations of Mg, the solubility of Si decreases even at pH values lower than 10. In this system, the dissolved ions precipitate as Mg-silicate (Wey and Siffert 1961). The pH values of groundwater in ophiolitic terrains are in general high, due to the presence of Mg-$HCO_3$. For example, Neal and Stanger (1985) reported groundwater with pH values of 11.2–11.6 in the region of Oman ophiolites. Similar high pH values are expected in the Eskişehir area, which is underlain by ophiolite; therefore, the results of Wey and Siffert (1961) are applicable to the sepiolitization process in the mixed-water zone in the Eskişehir area.

## CONCLUSIONS

In the Eskişehir area, magnesite pebbles in lacustrine conglomerates are partially to totally sepiolitized. This process of increasing sepiolitization of magnesite pebbles has been documented through XRD, chemical, SEM and $N_2$-BET techniques. In contrast to the sepiolitization of the magnesite pebbles deposited in a near-shore lake environment, no sepiolitization is observed in the sedimentary magnesite beds in the central part of the basin. The lack of sepiolitization in the central part of the basin is explained by the presence of pore waters, which were saturated with respect to magnesite. The sepiolitization in the near-shore lake environment is caused by the interaction of the mixed saline lake water and fresh ophiolitic water with the magnesite pebbles. The mixed waters were probably slightly undersaturated with respect to Si, which explains the partial sepiolitization of the magnesite pebbles. Furthermore, during this process the system was closed to $CO_2$. The experimental results of Wey and Siffert (1961) suggest that the sepiolitization of magnesite pebbles took place at a pH of about 11.0–11.5 in shallowly buried sediments. The necessary Si for sepiolitization in the mixed-water zone came from lake water during highstand episodes, when the magnesite pebbles in the near-shore environment were flooded. The chemical replacement process of magnesite by sepiolite is explained through a dissolution controlled-neomineralization model involving stages of dimerization, tetramerization, polycondensation and polymerization.

## ACKNOWLEDGMENTS

My thanks are extended to R. Ferrell, N. Güven, R. Hay, A. Okay and F. Çoban for their productive suggestions and critical review comments to improve the quality of the manuscript. The writer gratefully acknowledges A. Alkan and A. N. Coşkun of LASSA Tire Co. for the use of their SEM laboratory for this project.

## REFERENCES

Akıncı Ö. 1967. Eskişehir I24-c1 Paftasının Jeolojisi ve Tabakalı Lületaşı Zuhurları (Geology of Map I24-C1 area and bedded sepiolite exposures in Eskişehir). MTA Dergisi 67: 82–97.

Asutay HJ, Küçükkayman A, Gözler MZ. 1989. Dağküplü (Eskişehir Kuzeyi) Ofiyolit Karmaşığının Stratigrafisi, Yapısal Konumu ve Kümülatlarin Petrografisi (Stratigraphy and Structural Setting of Dağküplü Ophiolite Complex (North of Eskişehir) and Petrography of Cumulates). MTA Dergisi 109:1–8.

Badiozmani K. 1973. The dorag dolomitization model—Application to the Middle Ordovician of Wisconsin. J Sed Petrol 43:965–984.

Belzunce MS, Mendioroz S, Haber J. 1991. Activation of sepiolite from Vallecas-Vicalvaro deposit, Spain: Its influence on surface and catalytic properties. Proc 7th EUROCLAY 91 Conf; Dresden. 71–76.

Burnett WC. 1977. Geochemistry and origin of phosphorite deposits from off Peru and Chile. Geo Soc Am Bull 88: 813–823.

Dandy AJ, Nadiye-Tabbiruka MS. 1982. Surface properties of sepiolite from Amboseli, Tanzania, and its catalytic activity for ethanol decomposition. Clays Clay Miner 30:347–352.

Dandy AJ. 1968. Sorption of vapours by sepiolite. J Phys Chem 72:334–339.

Ece OI, Çoban F. 1994. Geology, occurrence and genesis of Eskişehir sepiolites, Turkey. Clays Clay Miner 42:81–92.

Ece OI. 1990. Geochemistry and occurrence of authigenetic phosphate nodules from the Desmoinesian cyclic Excello epeiric sea of the midcontinent, USA. Marine Petrol Geol 7:298–312.

Gibbs RJ. 1965. Error due to segregation in quantitative clay mineral X-ray diffraction mounting techniques. Am Mineral 50:741–751.

Gibbs RJ. 1968. Clay mounting techniques for X-ray diffraction analysis: A discussion. J Sed Petrol 38:242–244.

Imai N, Otsuka R. 1984. Sepiolite and palygorskite in Japan. In: Singer A, Galan E, editors. Palygorskite-sepiolite occurrences, genesis and uses. Dev In Sedimentol 37. Amsterdam: Elsevier. p 211–232.

Jones BF, Galan E. 1988. Sepiolite and palygorskite. In: Bailey SW, editor. Hydrous phyllosilicates. Miner Soc Am 19: Washington, DC. p 631–674.

Knauth LP. 1979. A model for the origin of chert in limestone. Geology 7:274–277.

Maliva RG, Siever R. 1989. Nodular chert formation in carbonate rocks. J Geol 97:421–433.

Neal C, Stanger G. 1985. Past and present serpentinisation of ultramafic rocks; an example from the Semail Ophiolite Nappe of northern Oman. In: Drever JI, editor. The chemistry of weathering. NATO Advanced Res Workshop. Holland: D. Reidel. p 249–275.

Riggs SR. 1979. Petrology of the tertiary phosphorite system of Florida. Eco Geol 74:195–220.

Serratoga JM. 1979. Surface properties of fibrous clay minerals (palygorskite and sepiolite). In: Mortland MM, Farmer VC, editors. Proc Int Clay Conf; 1978; Oxford. Amsterdam: Elsevier. p 99–109.

Singer A. 1989. Palygorskite and sepiolite group minerals. In: Minerals in soil environments. SSSA Book Series 1. Wisconsin. p 829–872.

Weaver CE. 1989. Clays, muds and shales. Devel Sedimentol 44. Holland: Elsevier. 819 p.

Wey R, Siffert B. 1961. Reaction de la Silice Monomoleculaire en Solution avec les ions Al, Mg. Genese et Synthese des Argiles. Colloque Int Centre Natl Rech Sci 105:11–23.

Yeniyol M. 1986. Vein-like sepiolite occurrence as a replacement of magnesite in Konya, Turkey. Clays Clay Miner 34: 353–356.

Yeniyol M, Öztunalı Ö. 1985. Yunak Sepiolitinin Mineralojisi ve Oluşumu (Genesis and Mineralogy of Yunak Sepiolites). In: Gündoğdu MN, Aksoy H, editors. II. Ulusal Kil Sempozyumu. p 171–186.

*(Received 21 March 1997; accepted 5 November 1997; Ms. 97-024)*